JOURNAL OF MATERIALS SCIENCE 29 (1994) 2944–2950

Ageing response and mechanical properties of a SiC_p/Al–Li (8090) composite

R. U. VAIDYA, Z. R. XU*, X. LI*, K. K. CHAWLA*, A. K. ZUREK
Materials Science and Technology, Los Alamos National Laboratory, Los Alamos, New Mexico 87545, USA
**Department of Materials Science, New Mexico Institute of Technology, Socorro, New Mexico 87801, USA*

The ageing kinetics of a silicon carbide particle-reinforced Al–Li (8090) matrix composite and unreinforced alloy, both made by spray forming, were investigated. Ageing treatments, without any straining after solutionizing, and with a 2% plastic strain after solutionizing, were employed. The peak ageing times of the matrix in the composite was shorter than that of the unreinforced alloy. The enhanced hardening rate of the matrix in the composite was attributed to the higher dislocation density induced as a result of the plastic deformation occurring at the particle/matrix interface. This plastic deformation is a result of the large difference in the coefficient of thermal expansion between the particles and matrix. Subjecting the samples to a 2% plastic strain reduced the peak ageing times even further. The tensile strength of the composite samples was marginally higher than that of the unreinforced alloy. Samples subjected to 2% plastic straining prior to ageing also exhibited higher strength values. The strain to failure of all the samples did not recover in the over-aged state.

1. Introduction

Composites consisting of aluminium matrices reinforced with ceramic particles are gaining in importance [1–5]. The ceramic particles increase the strength, stiffness, wear resistance and elevated temperature strength of the aluminium matrices. Unlike fibre-reinforced composites which exhibit severely anisotropic mechanical properties, particle-reinforced composites can have quite isotropic properties. Such aluminium matrix composites can also be shaped into their final configuration by conventional shaping techniques such as rolling and forging.

Aluminium–lithium alloys have gained increasing importance in recent years. This is because an addition of 2–3% of lithium to a conventional aluminium alloy increases the strength and stiffness, while at the same time reducing the density of the parent alloy [6, 7]. Developments in the spray-casting techniques and their adoption in ceramic particle-reinforced aluminium alloys have made it possible to produce Al–Li alloy matrix composites by a cospray method [8]. In this process, the molten alloy is atomized and the ceramic particles are introduced into the atomized metal stream. The high cooling rates obtained in the spray-forming process prevent segregation in the matrix, and produce a fine grain size, which is beneficial to the mechanical properties. Another possible advantage of the process is the relatively uniform distribution of the reinforcing particles obtained. Conventional casting techniques require stirring and mixing of the reinforcements into the molten matrix. If the wettability of the reinforcements by the matrix is low, which is usually the case in ceramic/metal systems, poor mixing and segregation of the particles can result. With the spray casting technique it is possible to overcome these disadvantages.

The presence of particle reinforcements have been shown to affect the ageing response of aluminium matrix composites as documented by Suresh & Chawla in a recent review [9]. This is because of the large difference in the coefficient of thermal expansion between particles and matrix. The thermal mismatch generates thermal stresses large enough to deform the matrix plastically, and induce a large dislocation density in the matrix. This large dislocation density has been shown [9] to accelerate the precipitation kinetics in this and other aluminium alloy systems. It can also affect the age-hardening behaviour in aluminium–lithium alloy composites.

Straining Al–Li alloys prior to ageing is beneficial in improving the strength and other mechanical properties of these alloys. The improved properties arise because of the modified chemistry of such alloys as a result of the addition of lithium. The primary strengthening phases in Al–Li alloys are Al_3Li, S′(Al_2CuMg), T_1(Al_2CuLi), and T_2(Al_6CuLi_3) [6]. All of these phases show a strong tendency to heterogeneous nucleation at dislocations and other structural inhomogeneities. Consequently, any kind of plastic deformation prior to ageing has a pronounced effect on the precipitation kinetics and distribution of the strengthening phases. It was of interest to study how the

0022–2461

plastic deformation applied to the composite samples could affect the ageing characteristics of such an Al–Li composite system. This was done by selecting two different ageing treatments: one without any straining of the samples prior to ageing, and the other with 2% straining prior to ageing. Tensile testing was done to determine the effect of ageing on the strength of the samples.

The objective of this work was to compare the ageing response of the unreinforced alloy and composite, with and without prestraining. The effect of ageing temperature and time on the tensile strength was also determined.

2. Experimental procedure

The nominal composition of the alloy is provided in Table I. Both unreinforced and reinforced alloy containing 15 vol % of silicon carbide particles (SiC_p) were studied. The samples were produced by a spray-casting technique (Osprey). The materials were obtained in the form of extruded billets, 0.45 m in length, and 0.075 m wide. The thickness of the billet was 0.0125 m. The extrusion process was carried out in one step at 538 °C, for 34 s, with an extrusion ratio of 17.1:1. The continuous extrusion pressure was 4.1 MPa.

Optical, scanning and transmission electron microscopy were used to characterize the microstructure. The grain size, volume fraction, and distribution of the SiC_p in the composite samples were also determined. Auger electron spectroscopy (AES) was used to obtain the elemental distribution. AES was carried out *in situ* on samples fractured in the microscope chamber.

Differential scanning calorimetry (DSC) was used to identify the precipitating phases. Rectangular samples ($1 \times 1 \times 0.5$ cm) were cut from the extruded stock, and heat treated according to the two treatments described below. A DuPont instrument (Model 2100) was used for the purpose. All of the DSC tests were carried out at a heating rate of 10 °C min^{-1}. The DSC runs were carried out in the temperature range of 25–600 °C.

Two different treatments were carried out on the unreinforced alloy and composite samples. In the first treatment, the as-received material was solutionized at 540 °C, water quenched and then aged at different temperatures (130, 150, 175 and 190 °C). In the second treatment, the samples were solutionized at 540 °C, quenched in water, aged at room temperature for 24 h, subjected to a 2% plastic strain, and then aged at 130, 150, 175, and 190 °C for specific periods of time. Vickers microhardness measurements, using 0.1 N for 10 s, were made on the unreinforced and reinforced materials to obtain the ageing curves. Tensile tests were done on dog-bone samples to evaluate the strength of the unreinforced alloy and composite samples after different heat treatments. Tensile testing was carried out in an Instron machine using a cross-head speed of 0.125 cm min^{-1}.

TABLE I Nominal composition of Al 8090 Alloy.

Element	Li	Cu	Mg	Zr	Fe	Si	Al
Composition (wt %)	2.2	1.1	0.5	0.12	0.08	0.04	Balance

3. Results and discussion

Low-magnification micrographs of the as-received composite are shown in Fig. 1a and b. The distribution of the particles was reasonably uniform as compared to similar composites produced by conventional

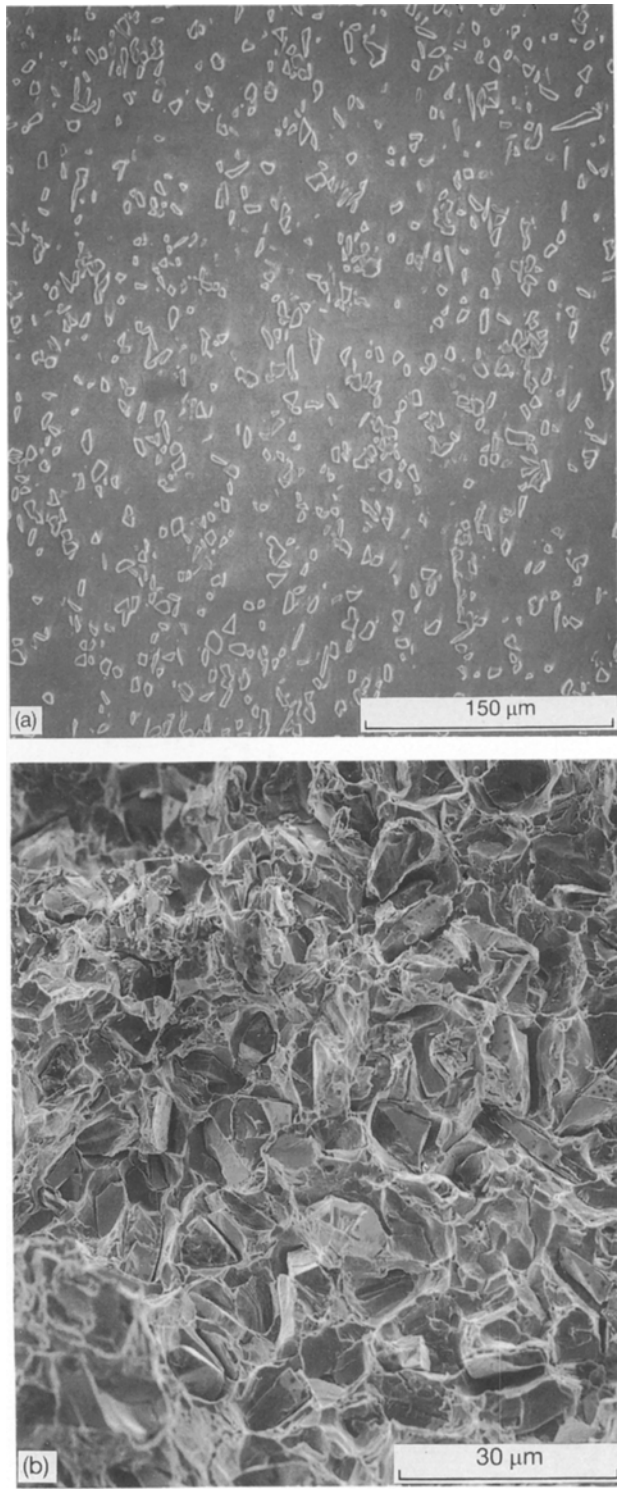

Figure 1 Low magnification scanning micrograph of (a) polished surface of SiC_p/8090 composite and (b) fracture surface of the composite. Note the size and distribution of the reinforcements.

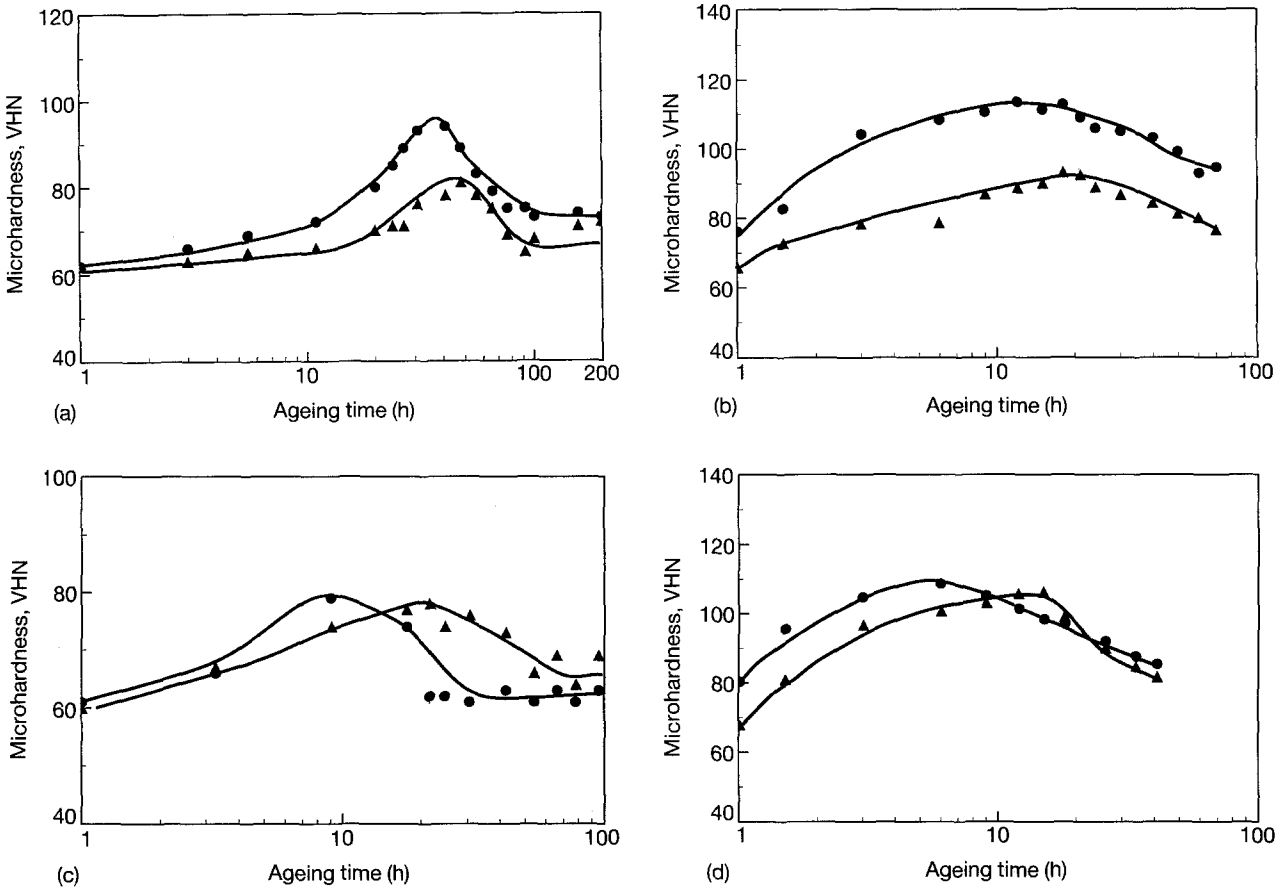

Figure 2 Ageing curves of the unreinforced alloy and matrix at different temperatures, without prestraining: (a) 130, (b) 150, (c) 175, (d) 190 °C. ▲, Al 8090; ●, SiC_p/Al 8090.

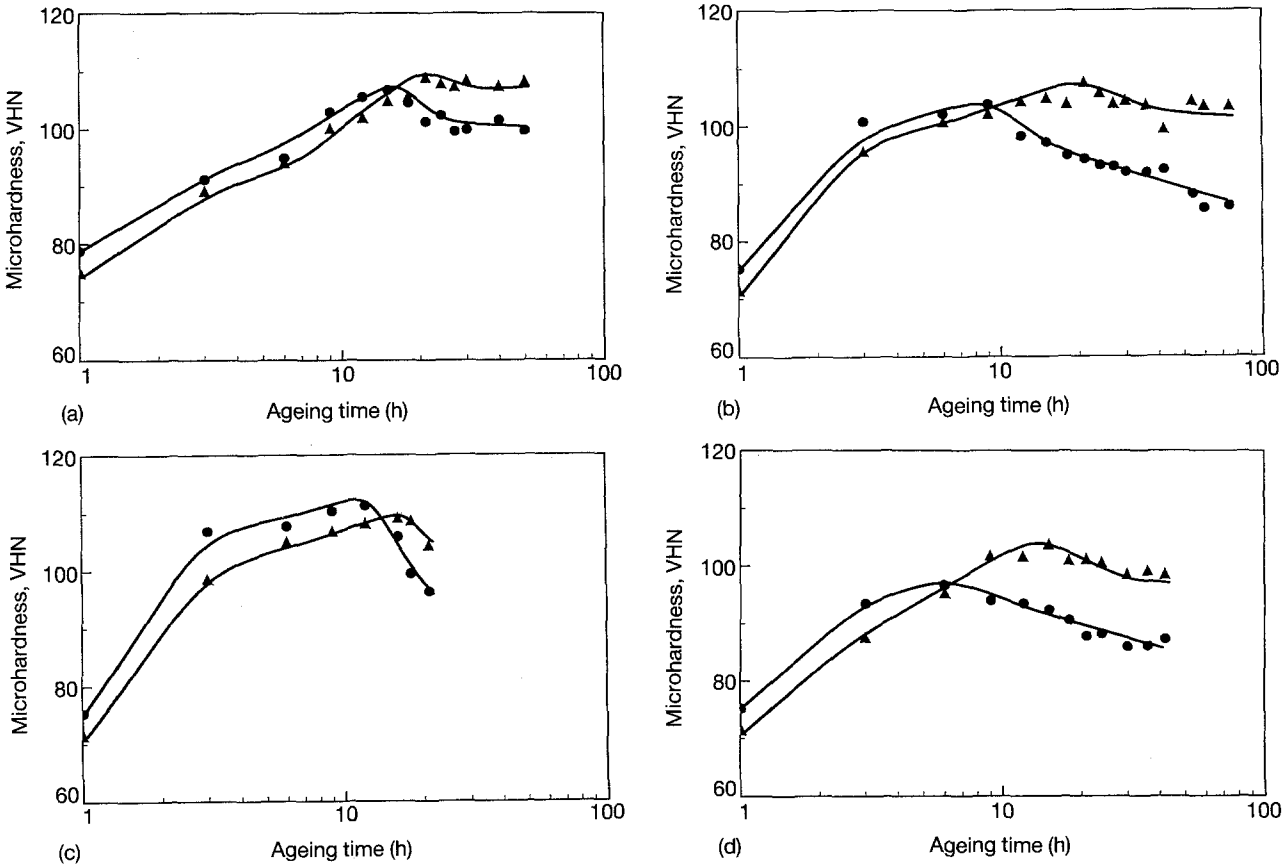

Figure 3 Ageing curves of the unreinforced alloy and matrix at different temperatures, subjected to a 2% plastic strain prior to ageing: (a) 130, (b) 150, (c) 175, (d) 190 °C. ▲, Al 8090; ●, SiC_p/Al 8090.

casting techniques. The volume fraction of the reinforcing particles determined by the lineal intercept technique was 15.1%.

The ageing curves of the unreinforced matrix and composite samples at four different temperatures (130, 150, 175 and 190 °C) for two different heat treatments are shown in Figs 2 and 3. The presence of the SiC_p accelerated the ageing kinetics of the matrix, especially at higher ageing temperatures. Plots of the time required to reach peak hardness against temperature, for the two heat treatments, are shown in Fig. 4a and b. Note that the difference in the time to peakage between the unreinforced alloy and composite samples decreased with decreasing ageing temperatures for both heat treatments. This is in accordance with studies done on a SiC_p/Al 2014 matrix composite [10]. At lower ageing temperatures, homogeneous nucleation of the GPB (Guinier–Preston–Berkenpas) zones dominates, while at higher temperatures heterogeneous nucleation of the precipitates dominates. Excess dislocations generated due to the mismatch in the thermal expansion between the matrix (21×10^{-6} $°C^{-1}$) and reinforcements (4.5×10^{-6} $°C^{-1}$), accelerate the ageing process. The excess dislocation density affects the ageing kinetics in the high-temperature ageing treatments more than in the low temperature ageing treatments. Also the time to peakage is signific-

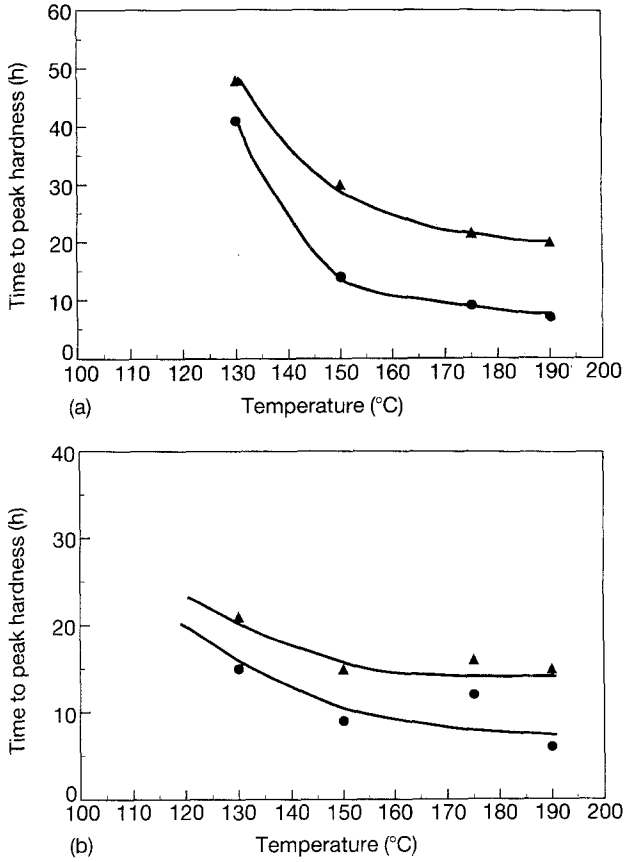

Figure 4 Time to peakage of the unreinforced alloy and matrix for: (a) samples without straining prior to ageing, (b) samples subjected to a 2% strain prior to ageing. ▲, Al 8090; ●, SiC_p/Al 8090.

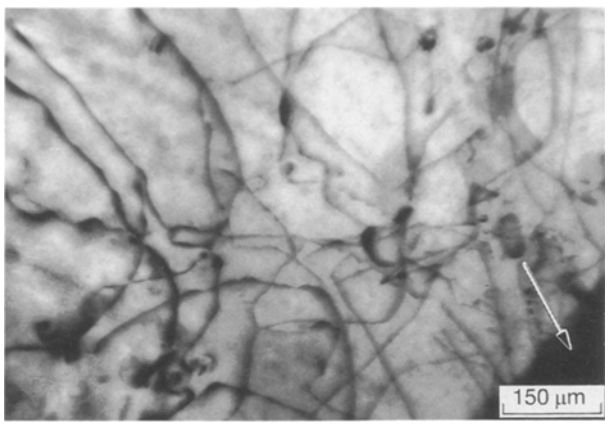

Figure 5 TEM micrograph of a composite sample illustrating the high dislocation density in the vicinity of the particle/matrix interface. Arrow denotes a SiC particle.

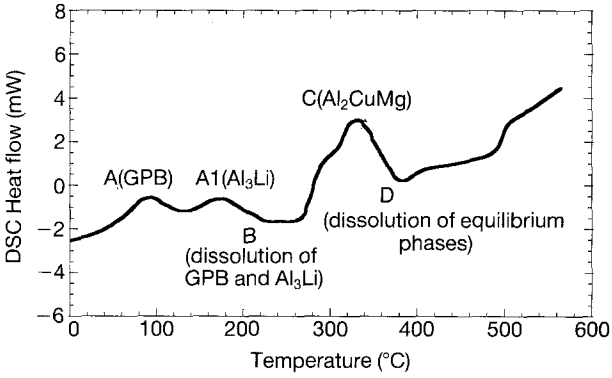

Figure 6 An ideal DSC curve of the 8090 alloy (at 10 °C min^{-1}) identifying the various peaks and precipitating phases associated with them.

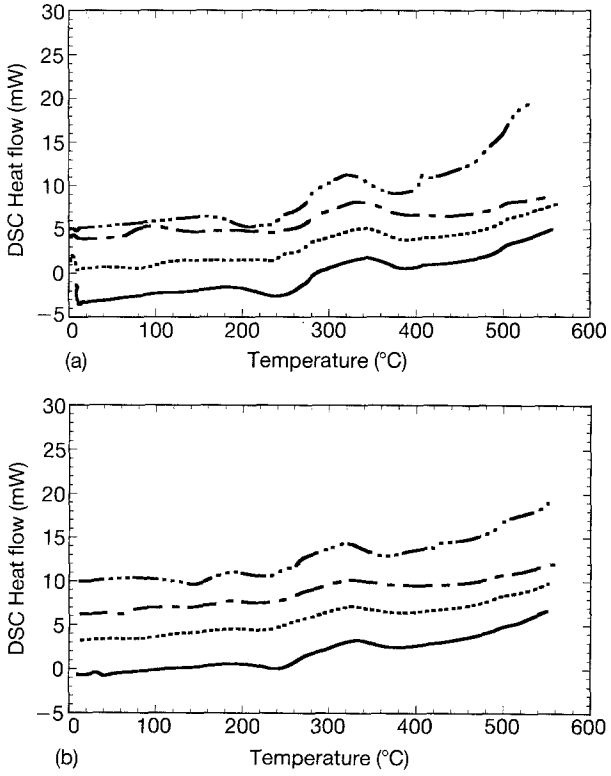

Figure 7 DSC curves of (a) the unreinforced alloy, and (b) composite samples subjected to various heat treatments. (——) HT 540 °C, WQ, aged at 190 °C for 8h; (- - -) HT 540 °C, WQ, aged at RT for 24h; (– – –) HT 540 °C, WQ; (— – —) as received.

antly smaller for both the unreinforced alloy and matrix in the composite, when subjected to the 2% strain prior to ageing. This is because of enhanced nucleation of the second phase at dislocations produced during prestraining.

The difference in the time to peakage between the unreinforced alloy and matrix is also smaller in the prestrained condition as compared to the unstrained condition, because of externally introduced dislocations. The transmission electron micrograph in Fig. 5 illustrates the high dislocation density in the vicinity of the particle/matrix interface.

One important observation which needs to be mentioned is that the hardness of the unreinforced alloy samples subjected to a 2% plastic strain, and aged at 130 and 190 °C, was greater than the matrix hardness under those conditions. In all the other cases, the hardness of the matrix in the composite was greater or equal to the hardness of the unreinforced alloy. We do not think this behaviour has any microstructural significance. This is because the trend observed in these two samples is not consistent with any one parameter (temperature or time, for instance). Also the difference in the hardness between the alloy and matrix is reasonably small (7 GPa) and is within acceptable experimental limitations.

An ideal DSC curve for the Al 8090 matrix is shown in Fig. 6 [11–15]. The precipitating phases corresponding to the various peaks have also been identified therein. Results of the DSC tests carried out on the unreinforced alloy and composite samples for various heat-treatment conditions are shown in Fig. 7a and b. Comparing these two figures reveals some interesting information. The peak C corresponding to the formation of the S′ phase is much larger in the unreinforced alloy than in the composite, whereas the A and A1 peaks are almost completely subdued in the composite samples. This indicates right away that S′ is the primary precipitating (and strengthening) phase in the composite. This is justifiable, based on the fact that the S′ phase primarily nucleates on dislocations and other inhomogeneities which are abundant in the composite as a result of the thermal stresses. On the other hand, Al_3Li and GPB nucleate homogeneously in the matrix, and do not require external nucleation sites. These DSC results corroborate the importance of the thermal stress-induced dislocations on the ageing kinetics of the system.

The strength of the unreinforced alloy and composite samples after the two heat treatments described earlier, with and without 2% prestraining, and aged at 130, 150, 175 and 190 °C, is given in Tables II–V, respectively. The strength of the composite samples was higher than the unreinforced alloy, but not significantly so. Also, the strength of the samples strained prior to ageing was higher than that of the unstrained samples. However the strain to failure of the composite samples was significantly lower as compared to

TABLE II Tensile strength of Al 8090 and SiC_p/Al 8090 at 130 °C.

Unstrained					2% Prestrained			
Condition	Unreinforced alloy		Composite		Unreinforced alloy		Composite	
	σ_f (MPa)	ε_f (%)	σ_f (MPa)	ε_f (%)	σ_f (MPa)	ε_f (%)	σ_f (MPa)	ε_f (%)
Underaged	292 (3 h)	10.4 (3 h)	307 (3 h)	9.65 (3 h)	295 (3 h)	8.6 (3 h)	307 (3 h)	4.15 (3 h)
Peakaged	325 (50 h)	7.8 (50 h)	332 (40 h)	3.55 (40 h)	333 (21 h)	6.25 (21 h)	335 (15 h)	3.53 (15 h)
Overaged	389 (72 h)	7.9 (72 h)	392 (60 h)	3.5 (60 h)	345 (36 h)	6.9 (36 h)	337 (24 h)	4.01 (24 h)

TABLE III Tensile strength of Al 8090 and SiC_p/Al 8090 at 150 °C.

Unstrained					2% Prestrained			
Condition	Unreinforced alloy		Composite		Unreinforced alloy		Composite	
	σ_f (MPa)	ε_f (%)	σ_f (MPa)	ε_f (%)	σ_f (MPa)	ε_f (%)	σ_f (MPa)	ε_f (%)
Underaged	373 (3 h)	8 (3 h)	394.2 (3 h)	5.5 (3 h)	392.7 (3 h)	6.3 (3 h)	396.4 (3 h)	4.1 (3 h)
Peakaged	409.6 (20 h)	4.2 (20 h)	456.7 (13 h)	3.9 (13 h)	460.7 (18 h)	3.8 (18 h)	469.4 (9 h)	2.8 (9 h)
Overaged	404.1 (72 h)	4.1 (72 h)	429.6 (72 h)	2.3 (72 h)	437.3 (72 h)	3.7 (72 h)	454.1 (72 h)	2 (72 h)

TABLE IV Tensile strength of Al 8090 and SiC_p/Al 8090 at 175 °C.

Unstrained					2% Prestrained			
Condition	Unreinforced alloy		Composite		Unreinforced alloy		Composite	
	σ_f (MPa)	ε_f (%)	σ_f (MPa)	ε_f (%)	σ_f (MPa)	ε_f (%)	σ_f (MPa)	ε_f (%)
Underaged	360.4 (3 h)	12.9 (3 h)	326.5 (3 h)	10.7 (3 h)	353.7 (3 h)	6.7 (3 h)	377.2 (3 h)	3.95 (3 h)
Peakaged	370 (24 h)	9.1 (24 h)	418.5 (9 h)	8.6 (9 h)	399 (16 h)	5.4 (16 h)	408 (12 h)	4.2 (12 h)
Overaged	307.4 (50 h)	6.1 (50 h)	314 (16 h)	7 (16 h)	356.8 (36 h)	6.3 (36 h)	386.6 (24 h)	3.93 (24 h)

TABLE V Tensile strength of Al 8090 and SiC_p/Al 8090 at 190 °C.

Unstrained					2% Prestrained			
Condition	Unreinforced alloy		Composite		Unreinforced alloy		Composite	
	σ_f (MPa)	ε_f (%)	σ_f (MPa)	ε_f (%)	σ_f (MPa)	ε_f (%)	σ_f (MPa)	ε_f (%)
Underaged	397.6 (3 h)	5.3 (3 h)	410.9 (3 h)	4.5 (3 h)	404.9 (3 h)	5 (3 h)	413 (3 h)	4 (3 h)
Peakaged	408.5 (18 h)	4.1 (18 h)	411.4 (7 h)	3.9 (7 h)	409.1 (16 h)	3.8 (16 h)	423.2 (6 h)	2.6 (6 h)
Overaged	398.8 (72 h)	5.1 (72 h)	399.8 (72 h)	3.5 (72 h)	410.1 (72 h)	3.1 (72 h)	420.1 (72 h)	2.4 (72 h)

Figure 8 Scanning micrograph illustrating lithium clusters (arrows).

the unreinforced alloy samples for all heat treatment conditions. The strain to failure of all the samples was also lowered when subjected to the 2% strain.

Over-ageing the samples, unreinforced or reinforced, did not lead to a recovery in the total strain to failure. One of the possible causes of this effect is that the SiC_p particles act as stress concentration sites and reduce the strength. It is possible for the reinforcing particles to crack or fragment during mechanical working. Frequently, these cracks are not readily visible, but can affect the mechanical properties. Another possibility is the clustering of lithium in the samples. Some such clustering was evident in the AES, and can be seen in Fig. 8. Clustering of Li can deplete the matrix of Li, and is detrimental to the overall mechanical properties. A third possibility is the magnitude of bonding between the particles and the matrix. The fractograph in Fig. 1 illustrates particle/matrix debonding. If the bonding between the particles and matrix is weak, inadequate load transfer will occur, and the strengthening observed in the composite is small. Further studies are in progress in order to more fully understand and determine the cause of this phenomenon.

4. Conclusions

The presence of the SiC particles accelerates the ageing kinetics of the Al–Li 8090 matrix as compared to the unreinforced alloy. The ageing kinetics of the matrix in the composite were much faster than those of the unreinforced alloy. The difference in time to peakage between the matrix and unreinforced alloy decreased with decreasing ageing temperature. This is

because at lower temperatures, homogeneous nucleation of GPB zones dominated, while at higher temperatures heterogeneous nucleation of the precipitates dominated. The differences in the time to peakage between the unreinforced alloy and composite samples was also smaller in the prestrained state as compared to the unstrained state. Straining the samples prior to ageing enhanced the process of heterogeneous nucleation as a result of the excess of dislocations generated in the samples. The tensile strength of the samples was not significantly affected by the prestraining treatment. Unlike microhardness, strength is a composite property and accounts for both the matrix and reinforcements.

Acknowledgements

The authors acknowledge the support of the Naval Surface Warfare Center, under contract No. N60921-91-M3678. The authors also thank Dr D. J. Lloyd of Alcan International and Dr A. Choudhary of Oak Ridge National Laboratory for their valuable help.

References

1. B. C. PAI, S. PAY, K. V. PRABHAKAR and P. K. ROHATGI, *Mater. Sci. Engng.* **64** (1976) 31.
2. R. J. ARSENAULT, *J. Mater. Sci.* **64** (1981) 171.
3. Y. FLOM and R. J. ARSENAULT, *J. Metals* **38** (1986) 31.
4. N. TSANGARAKIS, B. O. ANDREWS and C. CAVAILARO, *J. Comp. Mater.* **21** (1987) 481.
5. F. A. GIROT, J. M. QUENISSET and R. NASLAIN, *Comp. Sci. Tech.* **30** (1987) 155.
6. A. K. VASUDEVAN and R. D. DOHERTY (eds.), "Aluminium Alloys-Contemporary Research and Applications", Treatise on Materials Science and Technology, Vol. 31 (Academic Press, San Diego, 1989).
7. C. L. BUHRMASTER, D. E. CLARK and H. P. SMARTT, *J. Metals* **40** (1988) 44.
8. I. A. IBRAHIM, F. A. MOHAMED and E. J. LAVERNIA, *J. Mater. Sci.* **26** (1991) 1137.
9. S. SURESH and K. K. CHAWLA in "Metal Matrix Composites", (Butterworth–Heinemann, Stoneham, Massachusetts, 1993) in press.
10. K. K. CHAWLA, A. H. ESMAEILI, A. K. DATYE and A. K. VASUDEVAN, *Scripta Met. Mater.* **25** (1991) 1315.
11. A. K. JENA, A. K. GUPTA and M. C. CHATURVEDI, *Acta Metall.* **37** (1989) 885.
12. J. M. PAPAZIAN, C. SIGLI and J. M. SANCHEZ, *Scripta Metall.* **20** (1986) 201.
13. W. S. MILLER, L. A. LENSSEN and F. J. HUMPHREYS in "Aluminium–Lithium Alloys, V", Proceedings of the 5th International Al–Li conference, edited by E. A. Starke Jr. and T. H. Sanders Jr. (MCE, 1989) p. 931.
14. A. K. GUPTA, P. GAUNT and M. C. CHATURVEDI, *Phil. Mag.* **55** (1987) 325.
15. R. NOZATO and G. NAKAI, *Trans. Jpn. Inst. Metals* **18** (1977) 679.

Received 29 April
and accepted 6 October 1993